Development of Simultaneous Measurement System of Incipient Slip and Grip/Load Force
–Toward Dexterous Manipulations using Robot Hand Covered with Elastic Sensors–

Mitsunori Tada[1], Masakazu Imai[1], and Tsukasa Ogasawara[1]

Graduate School of Information Science
Nara Institute of Science and Technology
8916-5 Takayama-cho, Ikoma-shi, Nara, 630-0101, Japan
{mitsun-t, imai, ogasawar}@is.aist-nara.ac.jp

Abstract. This paper presents a simultaneous measurement system of incipient slip, which is considered to have explicit relation with force control, and grip/load force while human is grasping an object. The system composed of a transparent acrylic plate sustained by a 6-axis force-torque sensor, and a monocular camera inside the acrylic plate to observe contact region. We realize the measurement of incipient slip by tracking dot pattern drawn on the finger tip of the subjects. Measured data while subjects are lifting the device against external force under two frictional conditions are also presented. The experimental results suggest that: 1) contact mechanics of human finger have analogous tendency with that of elastic object, 2) the stick ratio has analogous profile even though the frictional condition (also, grip force) differs. These results are suggestive not only when clarifying mechanism of force control of human, but designing control criteria of robot hands covered with elastic tactile sensors.

1 Introduction

Robot hands have been expected to play an important role in flexible manipulations. And, they also have been thought to contain essential problems about both perception and motion control. From the beginning of robotics research, a considerable number of studies have been made on robot hands. In the beginning, stable prehension based on a precise object model [1], force control in grasping [2] and object recognition by tactile sensors [3] were hot research subjects, and many robot hands and tactile sensors were developed [4, 5]. However, traditional control criteria of robot hand were assuming point contact between robot hand and grasped object. As a consequence, robot hands were composed of rigid material and they possesses only position detectability as tactile sensation.

Recently, elasticity of human skin is thought to be indispensable for dexterous manipulations, so many researchers try to investigate and imitate intelligence of human hand and mechano-receptors in the skin. Hyun-Yong et al. have investigated mechanical property of finger tip and created artificial finger that has analogous mechanical property with human's [6]. Maeno et al. have calculated stress/strain distribution inside skin while being applied normal and tangential force using finite element method, and explain the sensibility of mechano-receptors in the glabrous skin [7]. Shinoda et al. have proposed acoustic resonant tensor cell which is composed of a small spherical cavity in a silicon rubber and can perceive principal stresses around the cavity using acoustic resonant frequency [8]. Moreover, Yamada et al. have proposed vibrotactile sensor which can distinguish only slipping state of grasped object by processing signals from PVDF transducer vertically standing near the surface of silicon rubber [9]. Though these types of sensors can give us predictive information of relative slip by sensing incipient slip between finger and grasped object, they have difficulty in doing theoretical analysis of grasping strategy. Since occurrence of incipient slip is based on a contact theory of elastic object which is much complicated than that of rigid object. On the other hand, human can manipulate various objects without any difficulty. Therefore, it is natural and important to design control criteria of robot hand covered with elastic sensors by observing and referring to the grasping motion of human.

With regards this point, physiologists have been investigating the dexterity of human hand by observing grasping motion. Johansson et al. have precisely investigated the relation between grip force and load force while grasping objects under variety of weight and frictional conditions, and ascertain that grip force has only small safety margin to prevent slips [10]. This skillful force control is thought to be realized by perceiving incipient slip inside contact region between finger and grasped object [11]. Also, if the

frictional condition of each finger differs in multi-fingered grasping, grip force of each finger also differs, since it is controlled according to local frictional condition, independently [12]. Moreover, Slinivasan et al. have investigated the response of SA and RA type of mechano-receptors by recording cutaneous impulse using microneurography while different textured objects are slipping on the finger tip [13].

Though many researchers have investigated intelligence of human hand and mechano-receptors, they were treating tactile sensibility and force control, separately. However, sensory input and motory output have explicit relation. So, in order to create novel control criteria of robot hands covered with elastic sensors, we must reveal the relation between sensory and motor skill of human.

In this research, we try to investigate dexterity of grasping motion by observing both sensory (occurrence of incipient slip) and motor skill (grip force and load force), simultaneously. This research can give us useful information regarding following two points.

1. We can directly investigate how human is adjusting their grip force according to sensory information, because we can observe incipient slip and grip/load force simultaneously.
2. We can determine what type of sensibility is needed for tactile sensors to control grip force according to frictional condition like human does, also we can create novel control criteria for robot hand covered with such sensors.

As a first step of this research, we propose a novel measurement device of grasping motion. The device can measure both incipient slip and grip/load force, simultaneously. Moreover, measured data while subjects are lifting the device against increasing external force in two frictional conditions are also presented.

This paper is composed of following sections. In Sect. 2, we explain why measurement of incipient slip is adequate for measurement of sensory skill of human, using theory of elastic contact and function of mechanoreceptors in the skin. In Sect. 3, we propose the measurement method of incipient slip and grip/load force, and explain the algorithm of image processing used in the measurement of incipient slip. In Sect. 4 we explain structure of the measurement device and experimental system. In this paper, we focus on measurement of precision grasp (grasp with thumb and index finger), so the device has two measuring sides. Finally in Sect. 5, we perform an experiment of lifting task of the device against increasing external force, and present the measured data of incipient slip and grip/load force, which give us suggestive information about force control of human.

2   Prediction of Relative Slip by Incipient Slip

2.1   Contact Mechanics of Elastic Object

According to the Hertz Theory (theory of elastic contact), shape of contact area between elastic object and rigid plate becomes ellipse as shown in Fig. 1, if the surface shape of the elastic object is approximately expressed as following equation [14].

$$z = Ax^2 + By^2 + Cxy + \cdots \tag{1}$$

Moreover, distribution of normal pressure inside contact area becomes hyperbolic paraboloid formulated as following equation,

$$\begin{cases} p(x,y) = p_0 \left(1 - \left(\frac{x}{a}\right)^2 - \left(\frac{y}{b}\right)^2 \right)^{\frac{1}{2}} \\ p_0 = \frac{3}{2} \frac{P}{\pi ab} \end{cases} \tag{2}$$

where P, p_0, a and b represent normal force, pressure at center of contact region, long radius and short radius of the ellipse, respectively. This theory takes no account of frictional force between elastic object and rigid plate, and assuming small deformation compared with dimension of the elastic object. However, Maeno et al. have revealed using finite element analysis that the distribution of normal pressure has analogous profile with that of Hertz Theory even though there exist frictional force and large deformation [7]. So we suppose that distribution of normal pressure between finger tip, which also possesses elasticity, and grasped rigid object is expressed by Hertz Theory.

Next, we try to apply tangential force to the finger while the finger is keeping contact with the rigid plate. If we suppose Coulomb's Law to describe contact mechanics between two objects, minimal
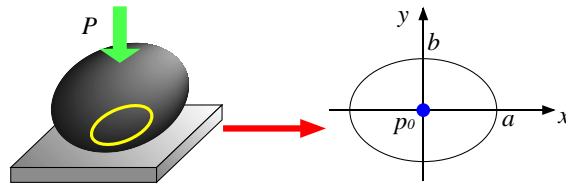
Fig. 1. Shape of Contact Area when Smooth Elastic Object Contact with Rigid Plate

tangential force which is needed to move (slip) partial region of contact area is formulated as following equation,

$$F_t = \mu F_n \tag{3}$$

where F_t, F_n and μ represent tangential force applied to the partial region, normal force applied to the partial region and frictional coefficient, respectively. So, if we try to increase the tangential force, boundary region of the contact surface, which has the smallest normal pressure, satisfies Equ. (3) and begins to slip at first. Moreover, if we continue to increase the tangential force, slipping area also continues to grow toward center of contact region. Finally the finger begins to slip relative to the grasped object when whole contact surface becomes slipping region. This phenomenon can be approximately expressed as Fig. 2.
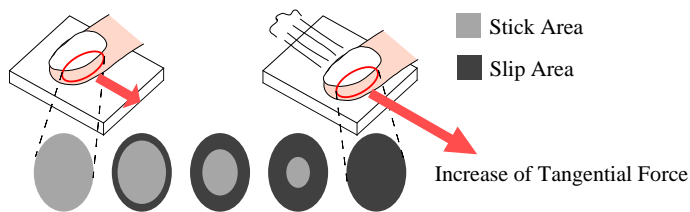
Fig. 2. Behavior of Contact Surface when Tangential Force is Applied

Partial slip which occurs before finger slips relative to the grasped object is called "incipient slip", and this phenomenon can give us predictive information of relative slip between finger and grasp object.

2.2   Perception of Incipient Slip by Mechno-Receptors in the Skin

Mechano-receptors in the skin cannot perceive incipient slip directly, since they are located several millimeter below the surface of the skin (Fig. 3). However, they can perceive acceleration, velocity or displacement around them [15] and therefore, they can be stimulated by the change of stress/strain distribution in the skin resulting from incipient slip. As evidences, John et al. have created mechanistic model of skin and predicted responses of SA (slowly adaptive) type mechanoreceptors against static stimulus by calculating state of stress and strain within the skin [16]. Srinivasan et al. have also calculate strain energy in the elastic body using finite element analysis and compared with the response of SA I type mechanoreceptors [17]. Moreover, Johansson et al. insist that FA I type mechanoreceptor is stimulated before relative movement of finger against grasped object, and the stimulus is caused by the incipient slip [11].

As explained in this section, incipient slip can supply predictive information about relative slip between finger and grasped object, and it can be perceived by mechanoreceptors located in the skin. Considering these facts, there must be explicit relation between occurrence of incipient slip and control of grip force. Therefore, we can obtain suggestive information about grasping skill of human by observing incipient slip and grip/load force, simultaneously.
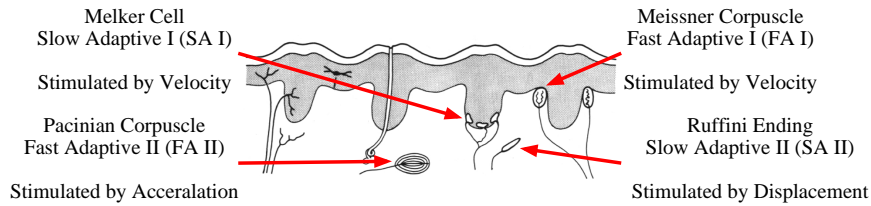
Fig. 3. Mechanoreceptors in Human's Glabrous Skin [16]

3   Simultaneous Measurement of Incipient Slip and Grip/Load Force

3.1   Measurement Method

A schematic of the measurement method is illustrated in Fig. 4. A transparent acrylic plate which will contact with finger tip is sustained by a 6-axis force-torque sensor, and a small CCD camera is fixed below the acrylic plate to observe contact surface. For this methodological reason, the measurement device must be transparent and rigid object. Moreover, the acrylic plate is illuminated from side area, so we can easily distinguish contact region by distraction light. If we suppose that there is only one contact area in one acrylic plate, we can calculate grip/load force, a moment normal to the acrylic plate and contact position using force and torque data measured from the sensor.

In order to measure incipient slip by image processing, there must be feature point to be tracked. Everyone possesses fingerprint as inherent pattern, so it is convenient to use it as feature point. However, there are following two problems.

– At finger tip, there are only 20 ∼ 30 feature points (branch or ending of fingerprint) per square centimeter. Moreover, the distribution of the feature point is not even.
– To find and track all the feature point of fingerprint is complicated problem and difficult to realize in real-time.

To realize reliable and real-time measurements, we draw a matrix of small dots on the finger tip, and use them as tracked features. Moreover, to avoid arbitrariness when selecting basis vector of the pattern (explained in Sect. 3.2), we draw larger three dots near the center of the pattern as shown in Fig. 4.
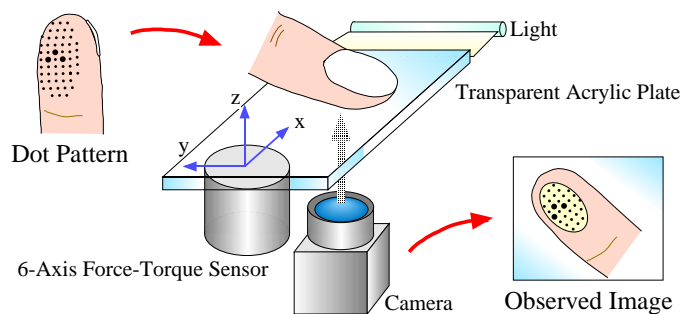
Fig. 4. Simultaneous Measurement Method of Incipient Slip and Contact Force

3.2   Image Processing to Measure Incipient Slip

The measurement of incipient slip is realized by tracking dot pattern drawn on finger tip. Though template matching based on calculation of correlation is popular technique in real-time image processing, it is difficult to apply it to our problem. Because, all targets (dots) have same shape, and are densely arranged in camera image. In this research, we propose fast and reliable tracking algorithm based on labeling operation. It is divided into following four operations.

1. Scaling down the camera image 0.2 times smaller. Applying binarization and labeling operation, and extract contact area. The threshold of the binarization is determined to maximize the variance between two classes.
2. Applying binarization and labeling operation to contact region determined in the former step, and extract position and area of all dots.
3. Arrange the extracted dots, and determine relative position of each dot (i.e. which dot is i-th in x direction, and j-th in y direction). We call this operation as "meshing" in this research. It is explained in Sect. 3.3.
4. Transform the position of dots from image coordinate C_i to sensor coordinate C_s (Fig. 4), by solving formula calculated from camera parameter (a 3×4 matrix which include both internal and external parameter of the camera) and constraint condition that all measured dots are on x-y plain of C_s.

We can realize real-time tracking of deformable dot pattern by these four operations, because we can simplify the problem in following two points.

– We can easily classify the dot, contact region and background by binarize operation, because contact region is emitting distraction light while other areas (dots and background) remain dark.
– Relative position of all dots never change by occurrence of incipient slip, because deformation of elastic material is continuous.

3.3   Algorithm of Meshing Operation

In this subsection, we propose the meshing algorithm which is taking account of feature of elastic contact. As a precondition, we suppose that there are total $(2m + 1) \times (2n + 1)$ (horizontal $\times$ vertical) dots drawn on the finger tip. The following explanation is only for quarter region of the dot pattern.

In the first step, we ascertain three larger dots near the center and define x and y-axis to satisfy following three conditions. (Fig. 5-(1)).

1. x-axis is on the longest edge of triangle composed of three larger dots.
2. y-axis is orthogonal to x-axis, and the rest dot (a dot that does not compose longest edge) is on the positive direction of y-axis.
3. x-axis and y-axis form right-handed system.

We also define the position of dot which is located ith in x direction, and jth in y direction as $\boldsymbol{r}_{i,j}$ ($i = -m, \cdots m, j = -n, \cdots n$). So, in this step, we've determined $\boldsymbol{r}_{1,0}$, $\boldsymbol{r}_{-1,0}$ and $\boldsymbol{r}_{0,1}$.

Second, we calculate estimated position of $\boldsymbol{r}_{0,0}$ and $\boldsymbol{r}_{0,-1}$ as following equation,

$$\begin{cases} \boldsymbol{r}_{0,0}^e = \left(\boldsymbol{r}_{1,0} + \boldsymbol{r}_{-1,0} \right)/2 \\ \boldsymbol{r}_{0,-1}^e = \boldsymbol{r}_{0,0} + \left(\boldsymbol{r}_{0,0} - \boldsymbol{r}_{0,1} \right) \end{cases} \tag{4}$$

where super script e means estimated position. After that we ascertain a dot which is located nearest to each estimated position, and determine them as $\boldsymbol{r}_{0,0}$ and $\boldsymbol{r}_{0,-1}$, respectively (Fig. 5-(2)).

Third, we calculate estimated position for $\boldsymbol{r}_{i,0}$ ($i = 2 \cdots m$) to satisfy following two equations,

$$\begin{cases} \angle \left(\boldsymbol{r}_{i,0}^e - \boldsymbol{r}_{i-1,0} \right) \cdot \left(\boldsymbol{r}_{i-1,0} - \boldsymbol{r}_{i-2,0} \right) = \angle \left(\boldsymbol{r}_{i-1,0} - \boldsymbol{r}_{i-2,0} \right) \cdot \left(\boldsymbol{r}_{i-2,0} - \boldsymbol{r}_{i-3,0} \right) \\ \left\| \boldsymbol{r}_{i,0}^e - \boldsymbol{r}_{i-1,0} \right\| = \left\| \boldsymbol{r}_{i-1,0} - \boldsymbol{r}_{i-2,0} \right\| \end{cases} \tag{5}$$

where $\angle \boldsymbol{v}_1.\boldsymbol{v}_2$ represents rotate angle from $\boldsymbol{v}_1$ to $\boldsymbol{v}_2$. Same as former step, we determine $\boldsymbol{r}_{i,0}$ as a dot which is located nearest to $\boldsymbol{r}_{i,0}^e$. This step is also applied for $\boldsymbol{r}_{0,j}$ ($j = 2 \cdots n$) (Fig. 5-(3)).

Finally, we regard $\boldsymbol{r}_{i-1,j} - \boldsymbol{r}_{i-1,j-1}$ and $\boldsymbol{r}_{i,j-1} - \boldsymbol{r}_{i-1,j-1}$ as a local basis vector pair of the dot pattern, and determine $\boldsymbol{r}_{i,j}$ ($i = 1 \cdots m, j = 1 \cdots n$) as the nearest dot of $\boldsymbol{r}_{i,j}^e$ defined as following equation.

$$\boldsymbol{r}_{i,j}^e = \boldsymbol{r}_{i-1,j-1} + \left(\boldsymbol{r}_{i-1,j} - \boldsymbol{r}_{i-1,j-1} \right) + \left(\boldsymbol{r}_{i,j-1} - \boldsymbol{r}_{i-1,j-1} \right) \tag{6}$$

Generally, we cannot uniquely determine the basis vector of dot pattern. But in this research, we can avoid this problem by making three larger dots (Fig. 5-(1)). Moreover, we can realize reliable tracking against deformable dot pattern, by changing the basis vector according to the deformation. That is, first we determine the position of dots which are located around the center where there is no slip, and after that meshing toward boundary area where there is large slip (deformation) changing basis vector of the dot pattern (Fig. 5-(4)).

If these four operations successfully finished, we can easily calculate deformation vector inside contact surface by subtracting corresponding dot position in referenced and current image. Therefore, we can distinguish slip area and stick area.
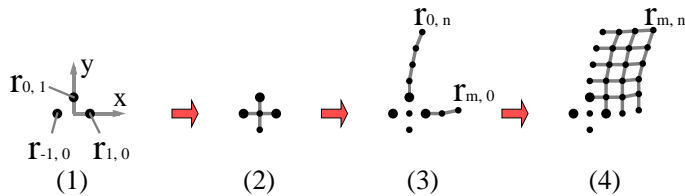
Fig. 5. Procedure of Meshing

3.4   Measurement of Grip/Load Force

We suppose that there is only one contact region in one acrylic plate, and the acrylic plate is on the plain which is spanned by x and y-axis of the sensor coordinate C_s (Fig. 4). We can calculate both grip force $\boldsymbol{f}_{grip}$ and load force $\boldsymbol{f}_{load}$ using measured three force, F_x, F_y and F_z, as follows,

$$\begin{cases} \boldsymbol{f}_{grip} = -F_z \boldsymbol{e}_z \\ \boldsymbol{f}_{load} = F_x \boldsymbol{e}_x + F_y \boldsymbol{e}_y \end{cases} \tag{7}$$

where $\boldsymbol{e}_i$ is a unit vector which direction is same as i-axis. Moreover, we can calculate contact position $(x, y)^T$ and contact moment m_z (moment at $(x, y)^T$ and around z-axis), using measured force F_i and moment M_i $(i = x, y, z)$. It is formulated as follows.

$$\begin{cases} x = -M_y/F_z \\ y = -M_x/F_z \\ m_z = -xF_y + yF_x + M_z \end{cases} \tag{8}$$

4   Development of Measurement Device and Experimental System

4.1   Structure of the Measurement Device

A structural figure and outward appearance of the developed device are illustrated in Fig. 6 and Fig. 7, respectively. In this research, we mainly focus on observation of precision grasp (pinch grasp using thumb and index finger), so the device has two measuring sides which are composed of a transparent acrylic angle sustained by 6-axis force-torque sensor (nano 4/5-s15: supplied by BL-Autotec). A small CCD camera (CK-200: supplied by KEYENCE), $\pi/4$ angled mirror and small halogen rump are installed inside the acrylic angle of index finger side to observe occurrence of incipient slip inside contact surface.

Dimension and weight of 6-axis force-torque sensor, CCD camera and the developed device are illustrated in Table. 1. Both sensors are small and light, so we can develop a measurement device which is small and light enough to be pinch grasped by human.

Table 1. Dimension and Weight of the Sensors and the Measurement Device

	Dimension ($\phi \times$H or D$\times$W$\times$H)	Weight
6-Axis Force-Torque Sensor	$\phi 17 \times 22$ [mm]	35 [g]
CCD Camera	$15.2 \times 31.2 \times 25.4$ [mm]	25 [g]
Developed Measurement Device	$59 \times 46 \times 130$ [mm]	270 [g]

4.2   Structure of the Experimental System

Structure of the developed experimental system is illustrated in left part of Fig. 8. The measurement device is fixed on a vertically standing slide guide. Upper part of the device is connected to exchangeable
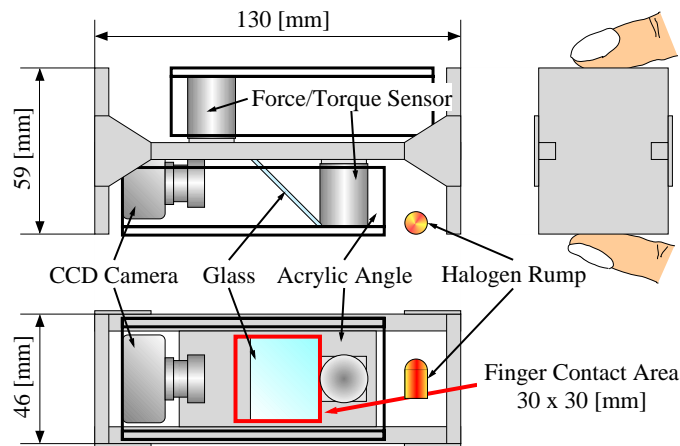
Fig. 6. Structural Figure of the Measurement Device
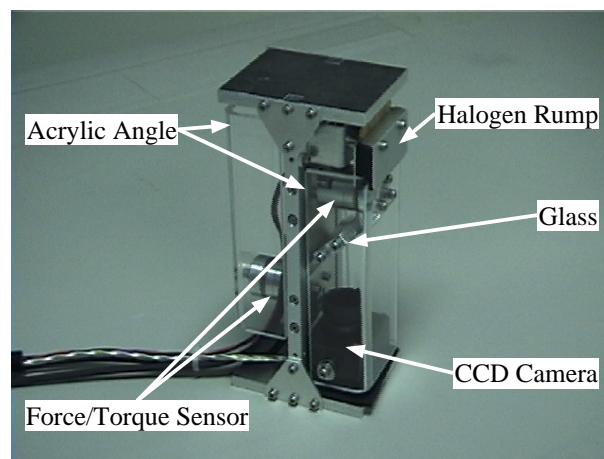
Fig. 7. Outward Appearance of the Device

load with steel wire via pulley, so we can setup several weight conditions by exchanging the load. We can also change the external force condition, by connecting lower part of the device and frame of the system with coil spring, Moreover, we can change frictional condition by coating surface of the acrylic plate with Vaseline. In the experiments, incipient slip and force/torque data are sampled, while subjects are trying to pinch and lift the device under arbitral weight, external force and frictional condition. Currently available experimental conditions are summarized in Table. 2.

The measurement system is connected to a host PC which possesses dual Pentium III processors, Linux2.2.14 / RT-Linux2.0 as an operating system and two PCI boards.

Basic image processing (zooming, binarization and labeling) are computed using versatile image processing board (IP5000: supplied by HITACHI), and meshing operation explained in Sect. 3.3 and the transformation of coordinate system are computed by CPU. Force-torque data are sampled through 12 [bit] AD converter board (AD12-64: supplied by Contec), and converted to grip/load force, contact torque and contact position by CPU.

An image processing task is executed as a normal Linux task. It takes only 20[ms] to complete binarize, labeling, meshing and transformation of coordinate frames, even though there are more than 150 dots drawn on the finger tip (Correctly, the camera outputs NTSC format video image, so the sampling ratio of dot position is at most 30 [Hz]). The resolution of the measurement is about 50 [μm]. Grip/load force, contact moment and contact position are sampled at 400[Hz] by RT-Linux sampling task, and are transfer to Linux force sampling process through RT-FIFO. Composition of the measurement software is

Table 2. Available Experimental Conditions of the Measurement Device

Factor	Conditions
Weight	300 [g] (light), 600 [g] (normal) or 900 [g] (heavy)
Force	Spring (proportionally increasing force) or Nothing (normal)
Friction	Vaseline (slippery) or Nothing (normal)

illustrated in the right part of Fig. 8. Finally, we illustrate the specifications of the measurement system in Table. 3.
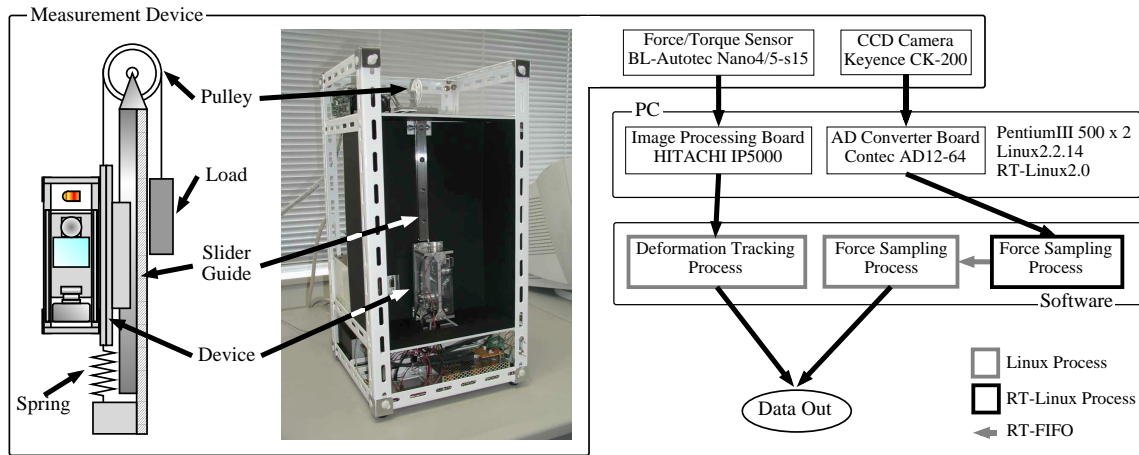
Fig. 8. Structure of the Experimental System

Table 3. Specification of the Experimental System

	Sampling Frequency	Resolution of the Measurement
Measurement of Incipient Slip	30 [Hz]	50 [μm]
Measurement of Grip/Load Force	400 [Hz]	0.032–0.098 [N]

5   Measurement of Grasping Motion under Two Frictional Conditions

5.1   Procedure of the Experiment

The experimental system explained in Sect. 4.2 is used in this experiment. We set up weight, force and frictional conditions as follows. Weight: 300 [g] (light) only, Force: Coil spring (proportionally increasing force) and Friction: Both normal and slippery conditions. Before the experiments, each subject has opportunity to try the experimental procedure until he/she is accustomed to the experiment, well.

In the initial state, the spring is relaxed. Subjects are instructed to pinch the measurement device with their thumb and index finger. Measured data of incipient slip, grip force and load force are sampled while subjects are lifting the device 200 [mm] from the initial position and return (it takes about $5 \sim 6$ [s]). The number of dots drawn on subject's finger tip are total $108 \sim 119$.

This experiment is aimed to know the following two points.

1. Behavior of contact surface while grasping an object.
2. Difference of incipient slip and grip force according to frictional condition.

5.2   Profile of Grip and Load Force in each Condition

The profile of grip force and load force in each condition are illustrated in Fig. 9 and Fig. 10, respectively. As we can see, grip force of thumb and index finger under slippery condition is higher than that of normal condition, while load force in both conditions are almost the same. This results coincide with Johansson's result [10].
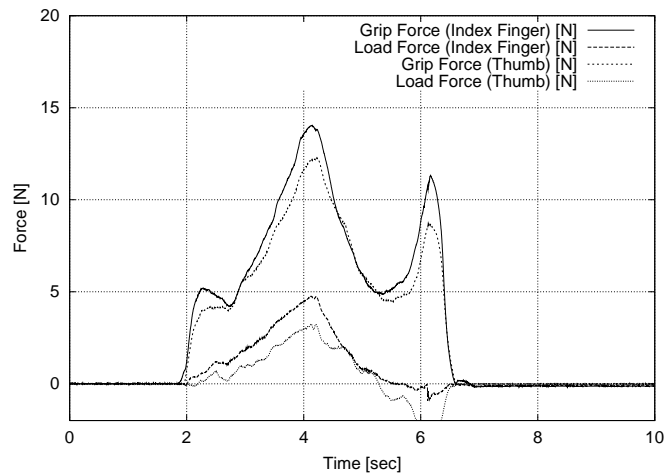
Fig. 9. Profile of Grip Force and Load Force under Normal Condition
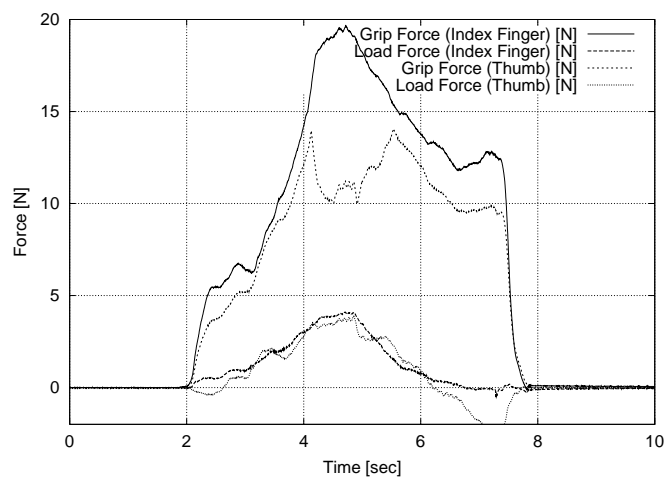
Fig. 10. Profile of Grip Force and Load Force under Slippery Condition

5.3   Occurrence of Incipient Slip

Processed images under normal condition are illustrated in Fig. 11, where (a) $\sim$ (d) represent the elapsed time after finger contact with the device.

Figure (a) is just after the finger contact with the measurement device (grip force only), while figure (d) is when the measurement device is 200 [mm] from initial position (maximum grasp force and load force are applied). Tangential force generated by the spring is applied to upward direction of the figure. By comparing (a) and (d), we can find out following two points.

(a) 0.0 [sec]   (b) 0.7 [sec]   (c) 1.4 [sec]   (d) 2.1 [sec]
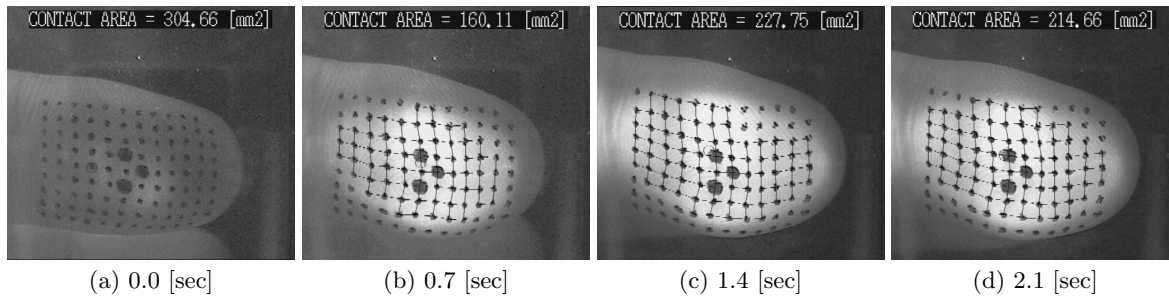
Fig. 11. Processed Image under Normal Condition

1. The boundary area of contact region is slipping to upward direction (same direction as tangential force).
2. The center area of contact region does not slip and keeps same position.

These two phenomena are well explained by a theory of elastic contact explained in Sect. 2.1. So, we can conclude that the contact mechanics of human finger has analogous tendency with that of elastic material. Also, proposed meshing algorithm, which is taking account of the feature of elastic contact, is effective to this problem.

5.4   Profile of Stick Ratio and Grip Force in each Condition

To compare the data of incipient slip in both conditions, we pay attention to the ratio of stick area (we call "stick ratio" in this research) in the contact region. Because stick ratio s, normal force P, tangential force Q and frictional coefficient μ are analytically expressed as following equation.

$$s = \left(1 - \frac{Q}{\mu P}\right)^{\frac{2}{3}} \tag{9}$$

This equation is obtained as a superposition of analytical pressure distribution in stick and slip region (Cattaneo's method), and known to satisfy boundary conditions of each region [14]. In Equ. (9) Q and μ are passively determined by condition of the measurement device determined in Sect. 5.1, while P and s correspond to grip force and sensory input, respectively. Therefore stick ratio s is adequate for representing contact situation of the finger.

Profile of stick ratio and grip force in each condition is illustrated in Fig. 12 and Fig. 13. Comparing Fig. 12 and Fig. 13, we can find out that the stick ratio in each condition has analogous profile, even though the frictional condition (also, profile of grip force) differs. This point is suggestive when considering skillful force control of human. That is, grip force is controlled optimally according to frictional condition.

6   Conclusion

In this paper, we present real-time measurement system of precision grasp, which can measure incipient slip, grip force and load force, simultaneously. We also present experimental results of lifting task under two different frictional conditions. Results of this paper are summarized as following three points.

– We proposed a tracking algorithm of dot pattern drawn on finger tip, taking account of the feature of elastic contact, and realized reliable and real-time measurement of incipient slip.
– We developed a simultaneous measurement device of incipient slip, grip and load force while grasping the device. The Incipient slip can give us predictive information about relative slip between finger and grasped object, and has explicit relation with force control. So, we can precisely investigate the mechanism of force control using this device.
– We performed an experiment of lifting task of the device under two different frictional conditions. The experimental results suggest that: 1) contact mechanics of human's finger tip have analogous tendency with that of elastic material, 2) stick ratio has analogous profile even though the frictional condition (also, grip force) differs.
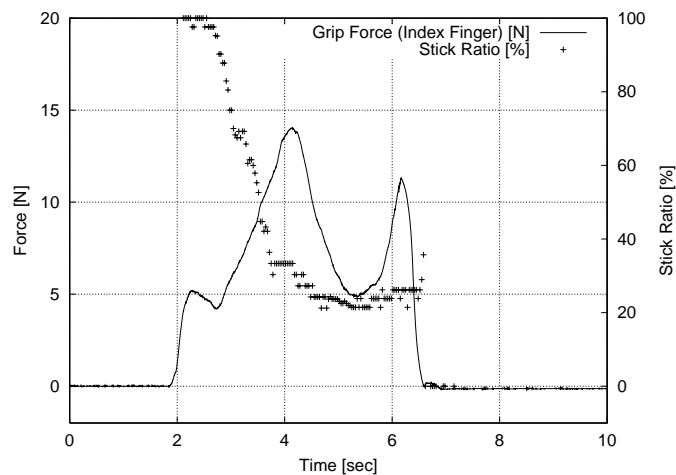
Fig. 12. Profile of Grip Force and Stick Ratio under Normal Condition
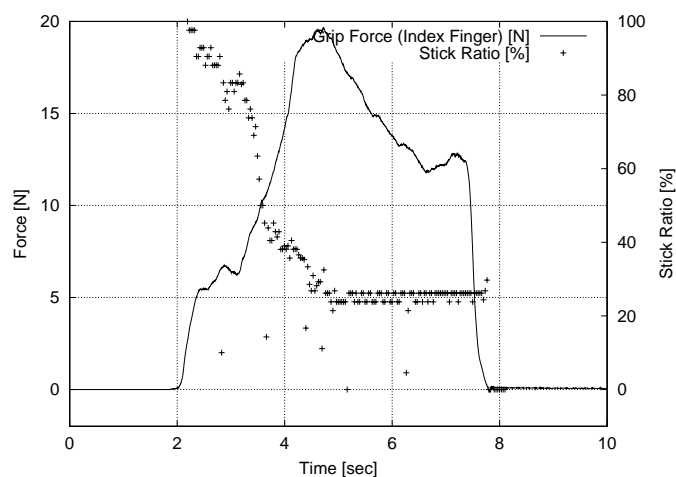
Fig. 13. Profile of Grip Force and Stick Ratio under Slippery Condition

In the future, we will perform experiments under various condition, and precisely investigate the relation between occurrence of slip and control of grip force. These experimental results will be useful not only when clarifying mechanism of force control, but designing control criteria for dexterous manipulation using robot hand covered with elastic tactile sensors.

References

1. H. Hanafusa et al. Stable prehension by a robot hand with elastic fingers. In Proceeding of 7th International Symposium on Industrial Robots, pages 361–368, 1977.
2. J. K. Salisbury et al. Articulated hands: Force control and kinematic issues. International Journal of Robotics Research, 1(1):4–17, 1977.
3. K. Nagata et al. Acquisition of an object model by manipulation with a multifingered hand. In Proceeding of IEEE/RSJ International Conference on Intelligent Robots and Systems, pages 1045–1051, 1996.
4. S. C. Jacobsen et al. Design of the utah/mit dexterous hand. In Proceeding of IEEE International Conference on Robotics and Automation, pages 1520–1532, 1986.
5. H.Maekawa et al. Development of a finger-shaped tactile sensor and its evaluation by active touch. In Proceeding of IEEE International Conference on Robotics and Automation, pages 1327–1334, 1992.
6. Hyun-Yong Han et al. Analysis of stiffness of human fingertip and comparison with artificial fingers. In Proceeding of the IEEE International Conference on SMC, pages 800–805, 1999.

7. Takashi Maeno, Kazumi Kobayashi, and Nobutoshi Yamazaki. Relationship between the structure of human finger tissue and the location of tactile receptors. JSME International Journal, 41(1):94–100, 1998.
8. Hiroyuki Shinoda, Kenichi Matsumoto, and Shigeru Ando. Acoustic resonatn tensor cell for tactile sensing. In Proceeding of the IEEE International Conference on Robotics and Automation, pages 3087–3092, 1997.
9. Yamada Yoji, Morita Hiroyuki, and Umetani Yoji. Vibrotactile sensor generating impulsive signals for distinguishing only slipping states. In Proceeding of the IEEE/RSJ International Conference on Intelligent Robots and Systems, pages 844–850, 1999.
10. G. Westling and R. S. Johansson. Factors influencing the force control during precision grip. Experimental Brain Research, 53:277–284, 1984.
11. R. S. Johansson and G. Westling. Roles of glabrous skin receptors and sensorimotor memory in automatic control of precision grip when lifting rougher or more slippery objects. Exp. Brain Res., 56:550–564, 1987.
12. M.K.O.Burstedt, J.R.Flanagan, and R.S.Johansson. Control of grasp stability in humans under different frictional conditions during multidigit manipulation. Journal of Neurophysiology, 82:2393–2405, 1999.
13. M. A. Srinivasan, J. M. Whitehouse, and R. H. Lamotte. Tactile detection of slip: Surface microgeometry and peripheral neural codes. Journal of Neurophysiology, 63(6):1323–1332, 1990.
14. K.L.Johnson. Contact Mechanics. Cambridge University Press, 1985.
15. Gordon M. Shepherd. Neurobiology. Oxford University Press, 1994.
16. Jonh R. Phillips and Kenneth O. Johnson. Tactile spatial resolution iii. a continuum mechanics model of skin predicting mechanoreceptor responses to bars, edges, and gratings. Journal of Neurophysiology, 46:1204–1225, 1981.
17. M. A. Srinivasan and K. Dandekar. An investigation of the mechanics of tactile sense using two-dimensional models of the primate fingertip. Transactions of the ASME, Journal of Biomechanical Engineering, 118:48–55, 1996.